Soil & Tillage Research 240 (2024) 106091

Contents lists available at ScienceDirect

Soil & Tillage Research

journal homepage: www.elsevier.com/locate/still

Does century-old biochar affect soil interrill erodibility on cropland soils? A study on pre-industrial kiln sites

M. Zanutel[a,*], A. Lefebvre[a], S. Garré[b], C.L. Bielders[a]

[a] Earth and Life Institute – Environmental Sciences, UCLouvain, Croix du sud 2, bte L7.05.02, Louvain-la-Neuve B-1348, Belgium
[b] Flanders Research Institute for Agriculture, Fisheries and Food (ILVO), Melle, Belgium

ARTICLE INFO

Keywords:
Biochar
Kiln site
Soil texture
Aggregate stability
Interrill erosion

ABSTRACT

Adding biochar to soils is being advocated to mitigate soil erosion. However, given biochar aging and persistency in soils, the effects of biochar on soil in the long-term are important to investigate yet remain largely unknown. The objective was therefore to determine the long-term effect of biochar on interrill erosion on cropland soils. Experiments were conducted using topsoil from three fields of different textures (silt loam, loam and sandy loam). Each field was characterized by the presence of kiln sites containing century-old charcoal used as proxy to investigate the long-term impact of biochar. Aggregate stability was measured using the method of Le Bissonnais (1996), whereas interrill erosion was studied using two successive (24-h apart) rainfall simulation experiments (84 mm h^{-1}, 90 min.). The presence of historical charcoal in kiln sites did not affect soil aggregate stability, irrespective of charcoal-C content or soil type. For the first rainfall simulation only, the century-old charcoal reduced both the final runoff and soil loss rates by, respectively, 15.4 mm h^{-1} and 12.1 g m^{-2} h^{-1} for each percent increase in charcoal-C content. As a result, Meyer's interrill erodibility decreased with increasing charcoal-C content. However, because the final runoff and soil loss rates decreased to a similar extent with increasing charcoal-C content, Kinnell's interrill erodibility was unaffected by charcoal-C content. These effects on interrill erosion parameters were independent of soil type and could not be related to changes in soil chemical properties. The measured reduction in runoff and soil loss were attributed to delayed crust development, which could be related to increasing proportions of clods in the soil samples with increasing charcoal-C content. Further research may be needed to confirm the observed trends and underlying mechanisms over a wider range of soil types.

1. Introduction

Soil erosion by water has been drawing much interest from the scientific community as well as from public and private stakeholders for many decades because of the sometimes severe on- and off-site consequences. On-site consequences include damage to crops, loss of soil organic matter and nutrients and, in the longer term, reduction of topsoil depth and overall capacity of soils to perform their ecosystem services (Boardman and Poesen, 2006). Off-site consequences comprise muddy floods, eutrophication of surface water as well as silting up of rivers or storm basins downstream (Verstraeten and Poesen, 1999; Boardman and Poesen, 2006; Boardman et al., 2006; Verstraeten et al., 2006). The annual cost of the loss in agricultural productivity due to soil erosion by water was estimated by Panagos et al. (2017) at around €1.25 billion at the European scale. These consequences and their high cost highlight the need for further research on practices to mitigate water erosion.

To reduce water erosion and its consequences, numerous management approaches have been developed and promoted (Evrard et al., 2010; Laloy and Bielders, 2010; Maetens et al., 2012). In general, practices that prevent erosion (e.g. planting of winter cover crops, conservation tillage) should be preferred over measures that mostly seek to reduce the off-site impacts (e.g., grass buffer strips, porous barriers). Preventive measures seek to maintain or improve soil infiltration capacity, protect the soil against direct drop impact as well as enhance soil aggregate stability and cohesion in order to reduce runoff and soil detachment. While ensuring a permanent soil cover is likely to be the most effective approach (Zuazo and Pleguezuelo, 2008), cropping systems with permanent cover remain marginal in the context of intensive agricultural systems in western Europe, and maintaining a permanent cover may not be easily applicable to all cropping systems. Hence there

* Correspondence to: Earth and Life Institute, UCLouvain, Croix du sud 2, bte L7.05.02, Louvain-la-Neuve, B-1348 Belgium.
E-mail address: martin.zanutel@uclouvain.be (M. Zanutel).

https://doi.org/10.1016/j.still.2024.106091
Received 10 March 2023; Received in revised form 1 October 2023; Accepted 13 March 2024
Available online 26 March 2024

is a need for soil amendments to prevent soil structure degradation or even to improve soil structure. Whereas the value of manure, compost or crop residues for improving soil structure is well established (Bronick and Lal, 2005), the use of these amendments may be constrained by environmental considerations (e.g., groundwater protection against leached nitrate), agronomic considerations (e.g., N immobilization by residues with high C/N ratio; disease control), or by local availability of the source material. In this context, the use of biochar is an additional promising avenue for soil erosion management (Blanco-Canqui, 2019; Gholamahmadi et al., 2023).

Biochar is a carbon-rich product derived from the pyrolysis of biomass such as livestock manure, sewage sludge, wood or crop residues (Lehmann and Joseph, 2015; Trupiano et al., 2017). Because of its long-term persistency in soils, the addition of biochar has been proposed as a way to mitigate climate change through carbon sequestration in soils (Lehmann et al., 2006; Woolf et al., 2010; Gupta et al., 2020). In addition to its carbon sequestration potential, previous studies have shown that biochar can improve soil quality and consequently crop performance (Jeffery et al., 2011; Biederman and Harpole, 2013; Ding et al., 2016; Blanco-Canqui, 2017; Palansooriya et al., 2019; Singh et al., 2022).

Regarding the effects of biochar on soil erosion, the review of Blanco-Canqui (2019) reported that biochar burial in soil reduces runoff by 5–50% and soil loss by 11–78% during rainfall events, whereas the meta-analysis of Gholamahmadi et al. (2023) highlighted that the addition of biochar to soil reduces runoff by 25% and soil loss by 16% on average. These effects were generally attributed to the positive impact of biochar on key soil properties which affect the runoff potential and soil erodibility (organic carbon content, hydraulic conductivity and aggregate stability, among others). However, it is worthwhile mentioning that negligible or even negative effects of biochar on soil loss have also been reported (Peng et al., 2016; Li et al., 2017; Lee et al., 2018; Zhang et al., 2019). Moreover, the extent of the reductions in soil erosion following the application of biochar appears to depend on numerous factors (e.g., biochar properties and application rate, initial soil properties, conditions of rainfall-runoff experiments, the presence of vegetation, type of climate), indicating that the effect of biochar application on soil erosion is context-dependent. For instance, the meta-analysis of Gholamahmadi et al. (2023) revealed that biochar was effective at mitigating soil erosion at gravimetric concentrations between 0.6% and 2.5%, whereas no significant effect was observed at lower and higher concentrations. Moreover, the reduction of soil erosion appeared much stronger in coarse-textured soils (Gholamahmadi et al., 2023).

While the short-term effects of biochar on soil erosion have been widely studied as reported in the previous paragraph, only Zanutel and Bielders (2023) have, to our knowledge, investigated its long-term effect on soil erosion. Studying this long-term effect is important given biochar persistency in soil (Lehmann, 2007; Solomon et al., 2007; Singh et al., 2012). Moreover, the properties of biochar particles change over time in soil, with a progressive fragmentation of these particles but also a progressive oxidation of the surface of these particles (the latter process is being referred to as biochar aging; Lehmann et al., 2005; Cheng et al., 2006). Biochar fragmentation and aging result in an increase in negative charges and a decrease in hydrophobicity of the surface of biochar particles (Cheng et al., 2008; Knicker, 2011; Criscuoli et al., 2014), properties that may directly affect soil erodibility.

Given the lack of long-term field experiments with biochar, the long-term effect of biochar can be investigated using kiln sites as natural model. Kiln sites are former charcoal production sites characterized by high concentrations of hardwood biochar (charcoal; from 1.8 to 33.1 g kg^{-1} on cropland; Hardy et al., 2016b) corresponding to leftovers of the charcoal production process dating back to the first half of the 19th century mainly (Hardy and Dufey, 2012). On bare soils, they are visible on aerial views as black patches a few decameters in diameter and are characterized by decreasing charcoal contents from the center outwards (Hardy and Dufey, 2015). Compared to adjacent reference (control) soils, previous studies demonstrated that kiln site soils on cropland are characterized by higher cation exchange capacity (CEC) and divalent exchangeable cation contents (Hardy et al., 2016b), which has been shown to favor organo-mineral associations and aggregation (Burgeon et al., 2021). We therefore hypothesized that biochar fragmentation and aging may also enhance its soil erosion mitigation potential. This was partly confirmed in a study by Zanutel and Bielders (2023), who reported lower runoff and sediment loss rates on soil from the center of kiln sites compared to reference soil for a sandy loam soil (but not for a silt loam soil). However, the latter study did not investigate the effect of century-old charcoal-C content on soil erosion.

The main objective of this research was therefore to characterize the long-term impact of biochar content on interrill erosion on cropland soils. In an approach similar to previous studies (Hardy et al., 2016a, 2016b; Burgeon et al., 2021; Zanutel et al., 2021; Zanutel and Bielders, 2023), samples taken at different distances from the center of kiln sites were used to study the long-term effect of hardwood biochar-C concentration in soils on interrill erosion-related properties of cropland soils. Soil chemical analyses, aggregate stability tests and rainfall-runoff experiments were performed to study the effect of charcoal-C content on interrill erosion-related properties. These properties were determined on different soil types, given that the effects of biochar are soil-dependent.

2. Materials and methods

2.1. Study sites and sampling

The three agricultural fields selected for this study were located in the municipalities of Gembloux (Silt loam region), Yvoir (Condroz region) and Attert (Belgian Lorraine) in Wallonia (Belgium; Fig. 1). In these areas, the climate is temperate oceanic (Table 1). Severe erosion on cropland and muddy floods are common place (Bielders et al., 2003; Verstraeten et al., 2006; Evrard et al., 2007). The soil at the study sites is classified as Luvisol (WRB classification) with a silt loam texture (USDA classification) in Gembloux, Cambisol with a loamy texture in Yvoir, and Planosol with a sandy loam texture in Attert (Table 1). The three fields are characterized by the presence of charcoal-enriched kiln sites visible on aerial photographs as black spots 20–25 m in diameter when the soil is bare (Fig. 1).

The selected fields were still covered with forest on the map of Ferraris (1770–1778), but no longer on the first official topographic survey map of the kingdom of Belgium (1865–1880). Therefore, deforestation most likely occurred during the first half of the 19th century, which also corresponds to the peak in charcoal production in Wallonia (Hardy and Dufey, 2012). In Wallonia, charcoal production took place in hornbeam and oak forests to meet the energy demands of the fast-growing steel sector prior to the switch to coal (Hardy and Dufey, 2012). Hence, the century-old charcoal particles are assumed to be dominated by oak and hornbeam at the three sites (Hernandez-Soriano et al., 2016; Hardy et al., 2016b, 2017).

Due to biochar fragmentation and aging over time in soils, the properties of charcoal particles from kiln sites are different than fresh biochar. This century-old charcoal has a high aromatic carbon content and a high cation exchange capacity estimated at 414 $cmol_c\ kg^{-1}$ of charcoal-C by Hardy et al. (2016b). Using X-ray photoelectron spectroscopy, Hardy et al. (2017) measured elemental contents ranging from 45.1% to 77.2% for C, from 17.4% to 42.2% for O and from 1.34% to 1.93% for N at the surface of charcoal particles from Belgian kiln sites. The surface of these charcoal particles was also characterized by low concentrations of Si (1.46–6.18%), Al (0.86–3.33%), Ca (0.23–1.75%) and Fe (0.16–1.22%). K and Mg were also detected at the surface of some charcoal particles. Hardy et al. (2017) also measured values of atomic H/C and O/C ratios for charcoal particles ranging from 0.57 to 0.77 and from 0.34 to 0.43, respectively. These ratios are higher than for fresh charcoal from active kiln sites (0.30 for H/C and 0.11 for O/C), reflecting among others a higher surface density of oxygen-rich

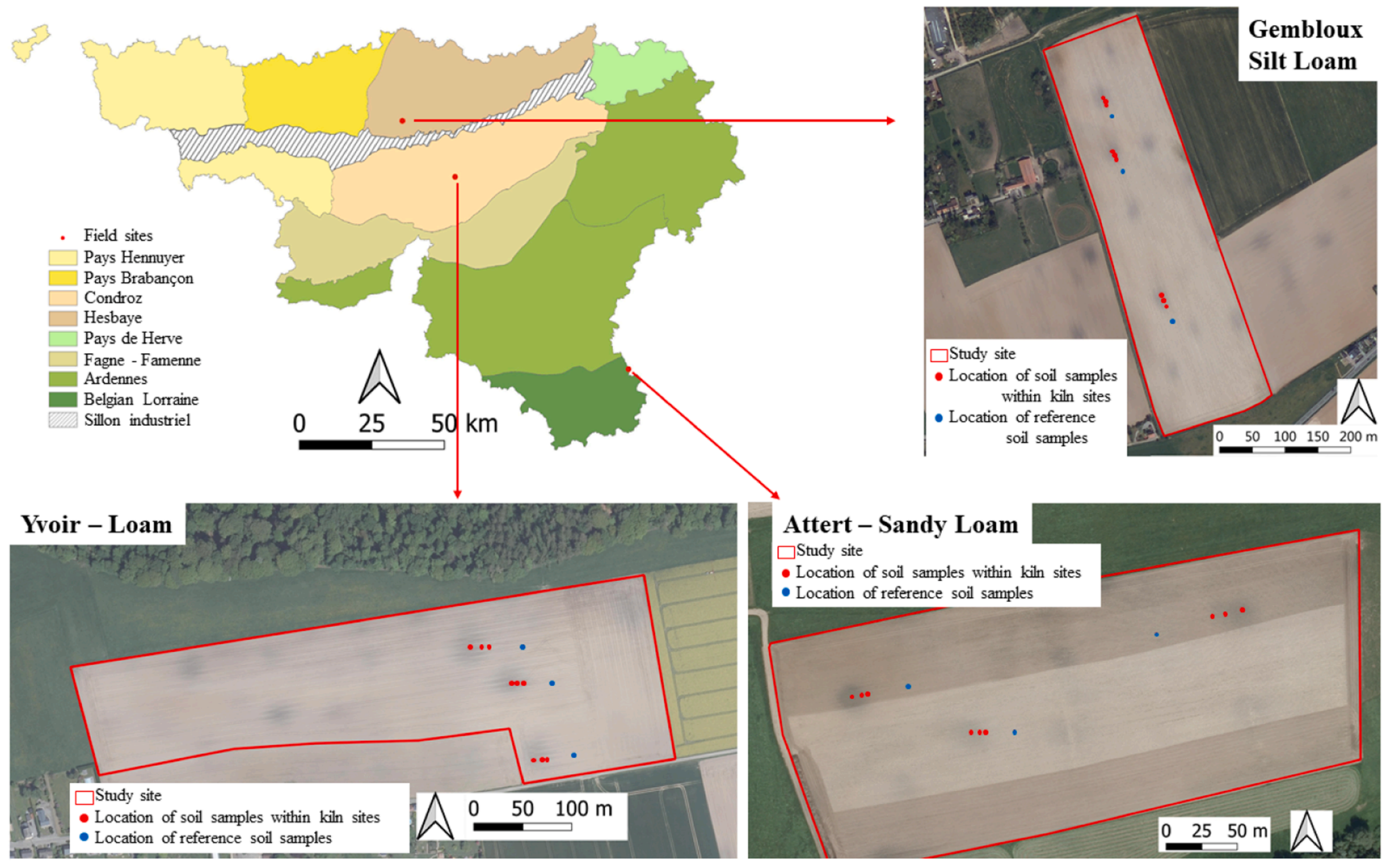

Fig. 1. Location of the study sites on the Belgian map of agro-geographic areas and aeral views showing the three sampling transects and sampling positions for the silt loam soil in Gembloux, the loamy soil in Yvoir and the sandy loam soil in Attert. Kiln sites are visible as darker black spots.

Table 1
Selected characteristics of the 3 study sites: municipality, latitude (Lat.) and longitude (Long.), 29-year (1991–2020) average annual temperature (Temp.) and precipitation (Prec.), average slope (Avg slope), gravel (> 2 mm), sand (50–2000 μm), silt (2–50 μm) and clay (< 2 μm) contents, textural class and soil type. For the gravel, sand, silt and clay contents, data are means ± standard errors of the means (n=3).

Municipality	Lat.	Long.	Temp.	Prec.	Avg slope	Gravel Content	Texture (USDA)				Soil type
							Sand	Silt	Clay	Text. Class(*)	
	N [°]	E [°]	[°C]	[mm]	[%]	[%]	[%]	[%]	[%]		(WRB)
Gembloux	4.75	50.52	10.2	793	0.5	1±0	5±0	80±1	16±0	SiL	Luvisol
Yvoir	5.00	50.35	9.6	902	2	13±4	35±5	48±5	16 ±1	L	Cambisol
Attert	5.82	49.74	9.1	1136	4	2±1	61±8	26±7	13±1	SaL	Planosol

(*) Textural classes: SiL = Silt loam, L = Loam, SaL = Sandy Loam.

functional groups such as carboxyl, carbonyl and O-alkyl (Hardy et al., 2017). More information on the chemical properties of century-old charcoal from Belgian kiln sites can be found in Hardy et al. (2017) and in Burgeon et al. (2021).

The soils at the three study sites have been cultivated conventionally, i.e., moldboard ploughing till 30 cm depth followed by one or more tillage operations for seedbed preparation. In Gembloux, a crop rotation was practiced, alternating between chicory, winter wheat, sugar beet, and potatoes, with winter cover crops when applicable (mustard and phacelia). In Yvoir, the crop rotation includes maize, sugarbeet, potatoes and winter grain, with winter cover crops when applicable. In Attert, the field has been cultivated continuously with maize, with winter cover crops.

Soil sampling occurred approximatively one month after sowing on the 25th of October, 8th of November and 15th of November 2019 in Gembloux, Yvoir and Attert, respectively. The preceding spring crops and the crops at the time of the sampling were chicory and mustard in Gembloux, sugar beet and winter barley in Yvoir, and maize and winter wheat (used as cover crop) in Attert, respectively.

Three charcoal kiln sites were selected on each field (Fig. 1). For each kiln site at each study site, the topsoil (0–10 cm) was sampled at three positions along a transect starting from the center of kiln sites and going outwards. Charcoal-C concentration will be highest for samples from the center of kiln sites and decreasing outwards (Fig. 1). In addition, reference soil samples were collected at a position located more than 20 m away from each selected kiln site on each study site (Fig. 1). These reference soil samples are assumed to be free of charcoal, although Hardy et al. (2016b) found small amounts of charcoal-C (0–2.6 g kg^{-1}) at such reference locations by means of differential scanning calorimetry. This was attributed to transport by tillage and other lateral transport processes.

For each sampling location at each study site, approx. 30 dm^3 of disturbed soil was sampled, air-dried and sieved at 2 cm for use in the rainfall-runoff experiments (most of the soil), and at 2 mm for the determination of soil chemical properties (a few grams). In addition to the disturbed soil samples, approx. 30 g of 3–5 mm soil aggregates were taken and air-dried for the determination of aggregate stability for each sampling location at each study site. At the time of sampling, soil bulk density did not significantly differ across sampling locations and study sites, with mean values of 1.37±0.02 g cm^{-3} (mean±standard error) at reference locations and 1.32±0.03 g cm^{-3} at the center of kiln sites.

2.2. Soil chemical properties

Chemical properties were determined for each sampling location on a few grams of air-dried soil sieved at 2 mm. A glass electrode was used to determine soil pH-KCl in a 1:5 (volume fraction) suspension of soil in 1 M potassium chloride solution (ISO 10390). Dry combustion was used to determine soil organic carbon (SOC; Vario MAX analyser, Elementar). Inorganic carbon content was negligible (below the limit of quantification).

Charcoal-C content was estimated by calculating the difference in carbon content between a given kiln site sample and the corresponding reference sample (Eq. 1).

$$\mathrm{Charcoal\_C_i} = \mathrm{SOC_i} - \mathrm{SOC_{ref}} \tag{1}$$

with $Charcoal\_C_i$ and SOC_i the charcoal-C and SOC contents at a position "i" in a kiln site [g kg^{-1}], respectively, and SOC_{ref} the SOC content from the corresponding reference sample [g kg^{-1}]. The limitations of this method were discussed in Zanutel et al. (2021).

A hexaminecobalt trichloride solution was used as extractant to determine soil CEC (ISO 23470). Available potassium (K^+), calcium (Ca^{2+}) and magnesium (Mg^{2+}) were extracted with a 0.5 M ammonium acetate – 0.02 M ethylenediaminetetraacetic acid (EDTA) solution at pH 4.65 with a 1:5 soil:solution volume ratio (Lakanen and Erviö, 1971) and measured by spectrophotometry.

2.3. Soil aggregate stability

Aggregate stability was determined for each sampling location on 5 g of air-dried, 3–5 mm aggregates with the method developed by Le Bissonnais (1996). This method involves three different treatments: fast wetting, slow wetting and mechanical breakdown. The fast wetting test predominantly assesses the sensitivity of soil aggregates to slaking and seeks to mimic aggregate breakdown during an intense rainstorm, whereas the slow wetting test mostly reflects the effects of micro-cracking and physico-chemical dispersion and seeks to mimic conditions during a gentle rain. The mechanical breakdown test assesses the cohesion of aggregates in response to mechanical stress. For each sampling location, all three tests were replicated 5 times (i.e., 60 measurements per test per study site). Details of the experimental protocols can be found in Le Bissonnais (1996).

After each of the three treatments, the soil material was transferred to a 50-μm sieve immersed in ethanol (wet-sieving). The >50 μm fraction was collected, placed in an oven (105°C, 48 h) and gently dry-sieved by hand on a column of six sieves: 2000, 1000, 500, 200, 100 and 50 μm. The mass percentage of each size fraction was determined. The <50 μm fraction is estimated from the difference between the initial mass and the sum of the six other fractions. Finally, the aggregate stability was determined by calculating the mean weight diameter (MWD [mm]) as follows:

$$\begin{aligned}\mathbf{MWD} = (&\mathbf{3.5\ x\ [\% > 2mm] + 1.5\ x\ [\%1 - 2mm] + 0.75\ x\ [\%0.5 - 1mm]} \\ &\mathbf{+ 0.35\ x\ [\%0.2 - 0.5mm] + 0.15\ x[\%0.1 - 0.2mm]} \\ &\mathbf{+ 0.075\ x\ [\%0.05 - 0.1mm] + 0.025\ x\ [\%} \\ &\mathbf{< 0.05mm])/100}\end{aligned} \tag{2}$$

2.4. Interrill erosion: rainfall-runoff experiments

In order to estimate interrill erodibility, rainfall-runoff experiments were conducted using a rainfall simulator and a flume at the Earth and Life Institute of UCLouvain in Belgium. The flume (Length 75 cm x Width 50 cm x Depth 50 cm) was designed similar to Liebenow et al. (1990), with a slope of 10%. The flume was filled with a 35-cm thick layer of sand on top of a 5-cm layer of gravel to allow free drainage. A 5-cm layer of air-dried soil from the experimental sites was then placed on top of the sand. The soil was sieved at 2 cm similarly to Guo et al. (2010) and Zhao et al. (2015) in order to mimic field soil conditions just after crop sowing (seedbed). Soil bulk density ranged between 1000 and 1200 kg m^{-3} before rainfall simulations.

The artificial rainfall was applied using two pressure nozzles placed 2 m above the flume. The intensity of the artificial rainfall was 84 ±4 mm h^{-1}, with a Christiansen homogeneity coefficient of 0.985. The mean drop diameter was 1.17±0.15 mm and the kinetic energy of the simulated rain was 10.6 J m^{-2} mm^{-1}.

For each sampling location, a first rainfall simulation was conducted for 90 min. The soil in the flume was then left to drain freely for 24 h before undergoing a second rainfall simulation of 90 min. Therefore, a total of 2 ×12 rainfall simulations were performed per study site. A photograph of the soil was taken at the end of each rainfall simulation to keep track of changes in soil surface conditions. Indeed, several studies have shown that soil surface conditions are indicative of surface hydrodynamic properties (e.g., infiltrability; Auzet et al., 1995, 2005; Cerdan et al., 2002; Malet et al., 2003). Runoff samples were taken every 5 min. during rainfall simulations and the runoff volume was determined by weighing. After 24 h of sedimentation and removal of the supernatant, these samples were placed in an oven (105°C, 48 h) and then weighted in order to determine the eroded soil mass. Final runoff rate was determined on the basis of the last 2–5 runoff samples, i.e., over the last 10–25 min. The longest possible time interval was used (with a max. of 25 min) for which there was no significant change in runoff rate based on the slope of the linear regression between runoff rate and time. The final soil loss rate was determined for the same time interval as the interval used for determining final runoff rate.

Interrill erodibility was determined based on two different empirical equations: Eq. (3) introduced by Meyer (1981) and used especially by Liebenow et al. (1990), and Eq. (4) proposed by Kinnel (1993). Kinnel's equation is adapted to transport-limited conditions whereas Meyer's equation applies to detachment-limited conditions (Assouline and Ben-Hur, 2006; Zhang et al., 2020).

$$\mathrm{Ki\ (Meyer)} = \frac{\mathrm{Di}}{\mathrm{I^2\ Sf}} \tag{3}$$

$$\mathrm{Ki\ (Kinnel)} = \frac{\mathrm{Di}}{\mathrm{I\ R\ Sf}} \tag{4}$$

with Ki the interrill erodibility [kg s m^{-4}], Di the final interrill soil loss rate [kg m^{-2} s^{-1}], I the intensity of the rainfall [m s^{-1}], R the final runoff rate [m s^{-1}], Sf a slope factor [-] given by 1.05 – 0.85 exp(-4 sin (θ)) and θ the slope angle [radians].

2.5. Soil surface conditions

Because of high variability in measured final runoff and soil loss rates but also large differences in surface conditions (crusting and presence of aggregates) at the end of the rainfall simulations, we investigated *a posteriori* whether final runoff (or soil loss) rates were related to surface conditions. For this purpose, each photograph taken at the end of the rainfall simulations was classified visually into 4 groups from A to D – irrespective of soil type and charcoal content – on the basis of the proportion of visible aggregates remaining in the crust at the end of the rainfall simulation. Group A corresponds to surface conditions with a lower degradation state (larger number of clods / weaker crusting) whereas group D corresponds to a more advanced state of degradation (fewer clods / more severe crusting), groups B and C corresponding to intermediate degradation states. Note that the classification of images was done separately for the two rainfall simulations based on the least / most degraded state in each of the two series. In other words, what was classified as 'A' or 'D' after the second rainfall does not match with what was classified as 'A' or 'D' after the first rainfall event because crusting continued to evolve between the first and second rainfall event. Fig. 2 provides representative photographs of the different groups after the first rainfall simulation. Because of technical issues, some images could not be exploited. Overall, 30 and 26 photographs were considered for the 1st and 2nd rainfall simulation, respectively. For the 1st rainfall simulation, 8, 9, 7 and 6 photographs were included in groups A, B, C and D, respectively. For the 2nd rainfall simulation, it was 5, 7, 6 and 6 photographs in groups A, B, C and D, respectively.

2.6. Statistical analyses

Data were managed and analysed using the MATLAB software (version 2020a) and R studio (version 4.0.4; 2021). Using the "fitlm" function of MATLAB, a linear model between each studied variable (MWD, R, etc.) and the corresponding charcoal-C content was fitted for each site separately as well as for all sites combined. The p-value on the slope coefficient of the linear regressions was used to determine if there was a significant effect of century-old charcoal-C content on the dependent variables. The "fitlm" function was also used in addition to the "predict" function of MATLAB to fit a linear model with 95% confidence intervals between the final runoff and soil loss rates.

To assess whether differences in measured or calculated variables could be explained by differences in soil surface conditions, a one-way ANOVA was performed using the "aov" function of R studio using the using the 4 surface condition classes as explanatory variables. The "aov" function of R studio was also used to perform a one-way ANOVA test in order to compare results between sites. Tukey's Honestly Significant Difference post-hoc test (HSD test) was performed for pairwise comparisons with the "TukeyHSD" function in R studio.

For each statistical test, the conditions of homoscedasticity (Levene test) and normality (visual inspection based on a Q-Q plot and a graph of the residuals distribution) of residuals were checked, assuming independence of the samples. Overall, an effect was considered significant when the p-value (P) was less than 0.05.

3. Results

3.1. Soil chemical properties

For the reference samples, the sandy loam soil had a higher SOC content (19.8±0.5 g kg^{-1}) than the silt loam soil (12.1±0.5 g kg^{-1}) and the loamy soil (14.7±0.3 g kg^{-1}; Table 2). At the center of the kiln sites, SOC content ranged from 15.9 to 17.0 g kg^{-1} in the silt loam soil, from 26.1 to 34.0 g kg^{-1} in the loamy soil and from 25.5 to 30.7 g kg^{-1} in the

Table 2
Soil chemical properties for the center of the kiln sites ('Kiln') and reference samples ('Ref.') for each of the three study sites. P corresponds to the p-value on the slope coefficient of the linear regression between a given soil chemical property and the charcoal-C content (n=12). P-values in bold indicate a p-value < 0.05. SiL corresponds to the silt loam soil in Gembloux, L to the loamy soil in Yvoir, and SaL to the sandy loam soil in Attert. SOC corresponds to the soil organic carbon, CEC to the cation exchange capacity and Exch. K^+, Ca^{2+}, Mg^{2+} to exchangeable potassium, calcium, magnesium contents, respectively. Data are means ± standard errors of the means (n=3).

		pH-KCl [-]	SOC [g/kg]	CEC [$cmol_c$ kg^{-1}]	Exch. K^+	Exch. Ca^{2+}	Exch. Mg^{2+}
SiL	Ref.	7.2 ±0.1	12.1 ±0.5	9.7±0.4	0.30 ±0.01	12.9±0.5	0.73 ±0.01
	Kiln	7.3 ±0.1	16.6 ±0.2	11.3±0.5	0.27 ±0.03	15.0±1.0	0.77 ±0.02
	P	0.5374	na*	0.1100	0.4407	0.0681	0.9557
L	Ref.	6.6 ±0.1	14.8 ±0.2	6.25 ±0.15	0.36 ±0.05	9.3±0.6	0.77 ±0.05
	Kiln	6.8 ±0.1	29.9 ±1.6	11.0±0.6	0.38 ±0.09	14.7±0.4	0.91 ±0.02
	P	0.4516	na*	**<0.0001**	0.6860	**<0.0001**	**0.0363**
SaL	Ref.	6.1 ±0.2	19.8 ±0.5	8.6±0.1	0.75 ±0.09	7.9±0.5	1.36 ±0.09
	Kiln	6.1 ±0.1	27.7 ±1.1	11.0±0.5	0.71 ±0.11	10.3±0.5	1.62 ±0.14
	P	0.8206	na*	**0.0002**	0.8870	**0.0258**	**0.0033**

*Given that charcoal-C contents are derived from SOC contents, the linear regression was not performed between charcoal-C content and SOC content.

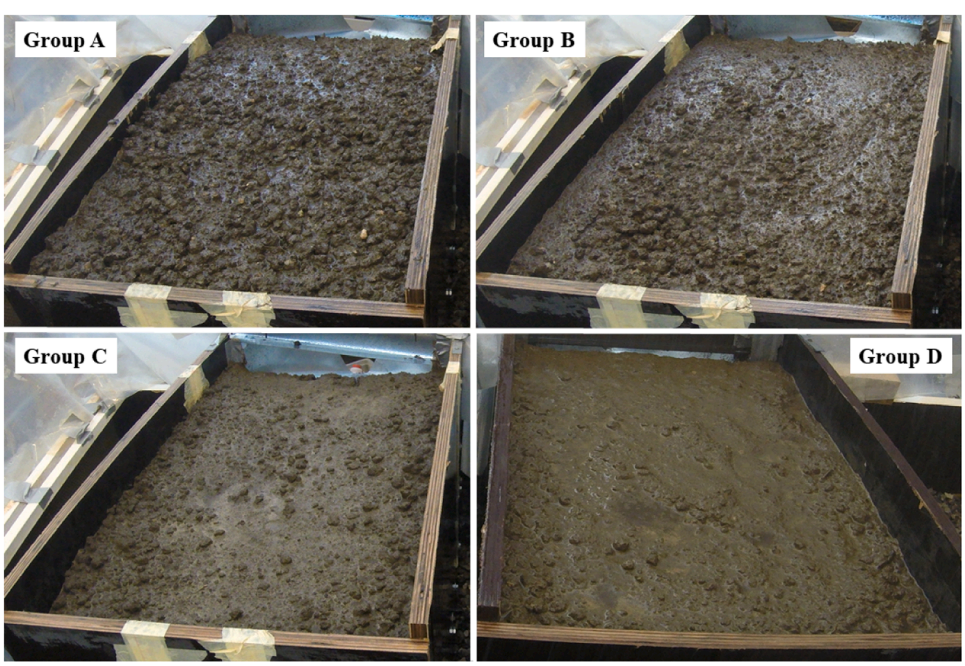

Fig. 2. Illustration of the soil surface conditions at the end of the first rainfall simulation for the 4 different groups (A to D).

sandy loam soil. As a result, the charcoal-C content at the center of the kiln sites was highest in the loamy soil (11.1–18.8 g kg^{-1}) and lowest in the silt loam soil (3.6–5.2 g kg^{-1}), with intermediate values for the sandy loam soil (6.6–9.9 g kg^{-1}).

pH-KCl was slightly acidic to neutral for all the study sites and unaffected by charcoal-C content (Table 2). Unlike exchangeable K^{+}, CEC and exchangeable Ca^{2+} and Mg^{2+} contents increased significantly with charcoal-C content for the loam and sandy loam soils. For the silt loam soil, charcoal-C content did not affect the measured chemical properties (Table 2).

3.2. Soil aggregate stability

For the reference soil samples, irrespective of the aggregate stability test (slow wetting, fast wetting or mechanical breakdown), the mean weight diameter of the aggregates was always higher for the loamy soil than for the silt loam soil (Fig. 3). For the sandy loam soil, the mean weight diameter of the reference samples was highest of all soils following the slow wetting test, intermediate for the fast wetting test and lowest of all soils for the mechanical breakdown test. For the loam and silt loam soils, the mechanical breakdown and slow wetting tests were almost equally destructive and less destructive than the fast wetting test. On the contrary, for the sandy loam soil, the mechanical breakdown test was almost as destructive as the fast wetting test, both tests being much more destructive than the slow wetting test.

Charcoal-C content did not significantly affect soil aggregate stability for any of the tests or study sites ($P > 0.05$; Fig. 4). Note that variability among replicate samples was high, especially for the slow wetting and mechanical breakdown tests.

3.3. Runoff and interrill soil loss

Final runoff rates varied from 2.5 to 60.8 mm h^{-1} for the first rainfall simulation experiment and from 13.9 to 82.9 mm h^{-1} for the second one (24 h later) across all sites and charcoal-C contents. The final soil loss rates ranged from 0.01 to 0.91 kg m^{-2} h^{-1} for the first rainfall simulation and from 0.05 to 0.52 kg m^{-2} h^{-1} for the second one. Overall, the final runoff and soil loss rates were linearly related (Fig. 5). There was no significant difference between study sites and between the first and second rainfall simulation.

Except for the silt loam soil during the second simulation, the general tendency was for final runoff and soil loss rates to decrease as a function of charcoal-C content (Fig. 6). Given that neither the slope nor the intercept of the linear regressions differed significantly across sites for

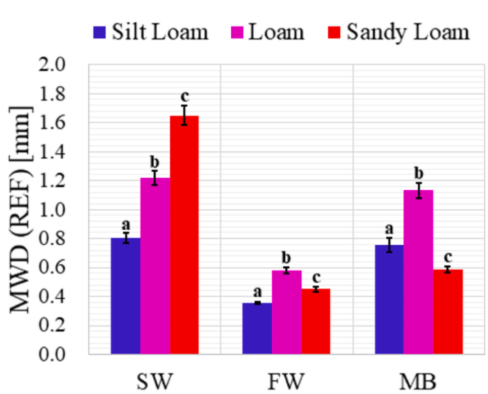

Fig. 3. Mean weight diameter (MWD) of aggregates from the reference (REF) soil samples for the silt loam (Gembloux), loam (Yvoir) and sandy loam (Attert) soils following the three tests of the method of Le Bissonnais: (a) SW = slow wetting, (b) FW = fast wetting, and (c) MB = mechanical breakdown. The error bars correspond to the standard errors of the means (n=15). P corresponds to the p-value of the ANOVA test. For a given test, bars marked with different letters are significantly different ($P < 0.05$).

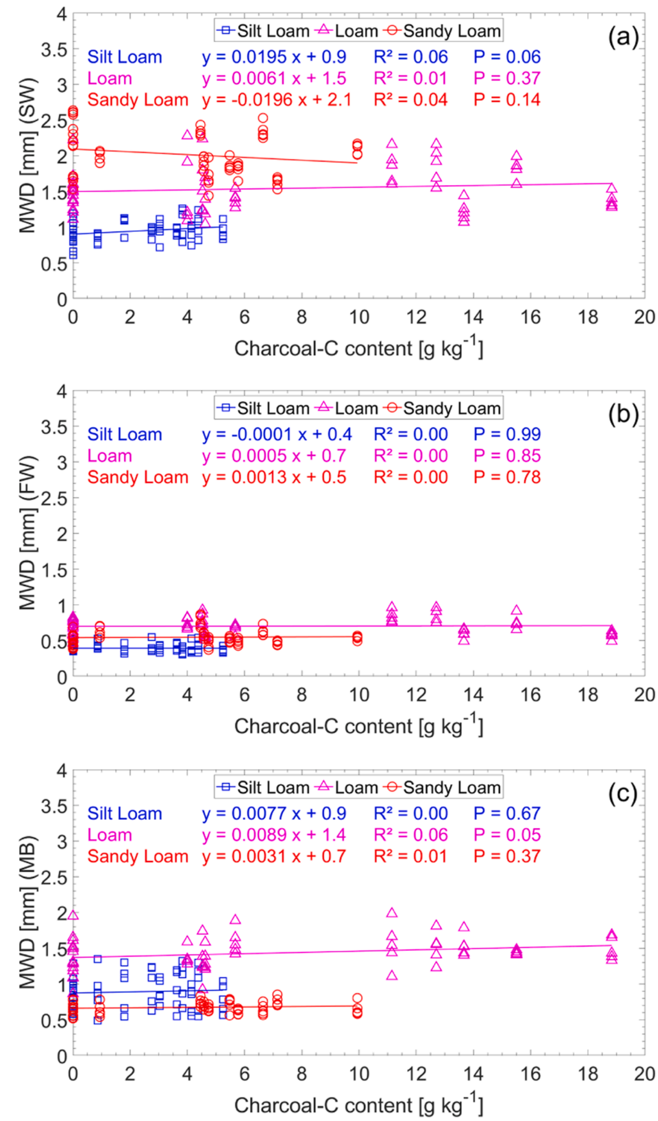

Fig. 4. Relationships between the mean weight diameter (MWD) of aggregates and the charcoal-C content for the silt loam (Gembloux), loam (Yvoir) and sandy loam (Attert) soils after having been subjected to one the three tests of the method of Le Bissonnais: (a) SW = slow wetting (b) FW = fast wetting (c) MB = mechanical breakdown. P corresponds to the p-value on the slope coefficient of the linear regressions (n=60 per study site).

both rainfall simulation experiments, a single regression between charcoal-C content and final runoff (or soil loss) rate was performed for all soils pooled together (Fig. 6). Overall, for the first rainfall simulation only, charcoal-C content significantly reduced final runoff ($P = 0.02$, Fig. 6a) and soil loss rates ($P = 0.05$, Fig. 6c). No such trend was observed for the second rainfall simulation 24 h later (Fig. 6b,d). Sediment concentration was not significantly affected by charcoal-C content (Fig. 6e,f).

3.4. Interrill erodibility

For the first rainfall simulation experiment only, the presence of century-old charcoal significantly reduced Meyer's interrill erodibility when all the measurements from the three sites were pooled together ($P = 0.05$; Fig. 6g). This reduction in erodibility with increasing charcoal-C content was not observed for Kinnel's interrill erodibility (Fig. 6i). For the second rainfall simulation, there was no significant effect of charcoal-C content on interrill erodibility, irrespective of the equation

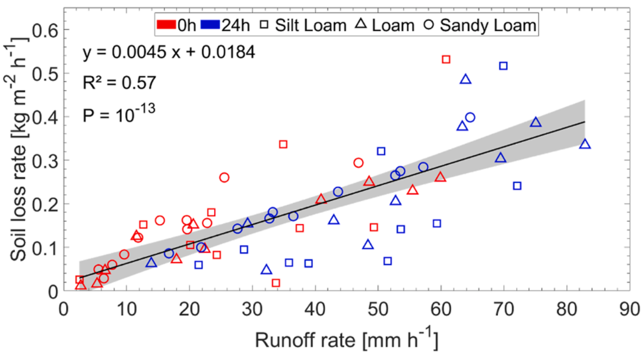

Fig. 5. Relationship between final runoff and soil loss rates. A linear regression model was fitted for all the data combined, given the lack of significant difference between the three study sites and between both rainfall simulations. 0 h and 24 h correspond to the first rainfall simulation and the second one (24 h later). P corresponds to the p-value on the slope coefficient of the linear regression (n=64). The shaded areas correspond to the 95% confidence intervals.

used (Fig. 6h,j).

3.5. Surface conditions

Measured and calculated variables from the first rainfall simulation were affected by the surface conditions, all study sites combined (Fig. 7). The more the surface is crusted and the fewer aggregates are present, the higher the final runoff rate (Fig. 7c), the final soil loss rate (Fig. 7e) and Meyer's interrill erodibility (Fig. 7 f). For the second rainfall simulation, only the final runoff rate was different from one group to another and therefore affected by the surface conditions (Fig. 7d). Charcoal-C content did not differ significantly across the 4 groups surface conditions (Fig. 7a,b), nor were the sediment concentration or Kinnel's interrill erodibility coefficient (not shown).

3.6. Correlations between variables

Interrill erosion parameters from the first rainfall simulation were negatively correlated with the mean weight diameter following the fast wetting and mechanical breakdown tests, all study sites combined (Table S1). However, only the correlations between sediment concentration or Kinnel's interrill erodibility and the mean weight diameter following the fast wetting test were significant. After the second rainfall simulation, these correlations were no longer significant, but a significant correlation was observed between the mean weight diameter after slow wetting and Kinnel's interrill erodibility (Table S1).

Due to the differences in soil chemical properties across study sites, correlations between soil chemical properties and interrill erosion parameters were investigated for each study site separately (Table S2). For the silt loam soil, the mean weight diameter after the slow and fast wetting tests was significantly and positively correlated with the exchangeable Ca^{2+} and Mg^{2+} contents, respectively. For the loamy soil, the mean weight diameter following the slow wetting test was significantly and positively correlated with pH-KCl. For the sandy loam soil, the mean weight diameter following the slow wetting test was significantly and negatively correlated with the exchangeable K^{+} content. Regarding the interill erosion parameters derived from the rainfall-runoff experiments, these parameters were not significantly correlated with soil chemical properties, except for the correlation between final runoff rate and exchangeable Ca^{2+} content on the silt loam soil. Overall, correlations between soil chemical properties and soil aggregate stability or interrill erosion parameters were weak and not consistent across sites.

4. Discussion

4.1. Effect of charcoal-C on soil chemical properties

The presence of century-old charcoal in kiln sites had no effect on soil pH, which is consistent with the observations of Hardy et al. (2016b). This lack of effect can be explained by the frequent liming of cropland, which seeks to keep soil pH within the optimal range for crop production, as well as by the progressive leaching of alkali and alkaline earth metal oxides present in biochar ash, which are responsible for the liming effect observed in the short-term after the addition of biochar to soils (Cheng et al., 2006).

Similar to the observations of Hardy et al. (2016b), the charcoal-C content increased the soil CEC and divalent exchangeable cation contents (Ca^{2+} and Mg^{2+}), most likely as a result of the high CEC of century-old charcoal particles. For the silt loam soil, the relationships between the charcoal-C content and these variables were, however, not significant, which may result from the lower charcoal-C content in the kiln sites of this soil compared to the loamy and sandy loam soils. Indeed, given the overall variability across samples, a smaller range in charcoal-C contents would hinder the detection of a possible significant trend.

4.2. Effect of charcoal-C on soil aggregate stability

Aggregates from the loamy soil were more stable than the silt loam soil for all the three aggregate stability tests. This could result from the higher uncharred organic carbon content and a lower silt content in the loamy soil compared to the silt loam soil. Indeed, it is well established that aggregated stability is positively correlated to organic matter content and negatively to silt content (Rivera and Bonilla, 2020). The uncharred organic matter can result in a reduction in the wettability and is an important binding agent of mineral particles, thereby favoring aggregate stability (Chenu et al., 2000). On the contrary, the presence of silt particles increases the sensitivity to slaking and dispersion, thereby reducing aggregate stability (Rivera and Bonilla, 2020).

Although the sandy loam soil had the highest uncharred SOC content and the lowest silt content (Table 1), aggregate stability was not systematically higher compared to the silt loam and loamy soil. Actually, aggregates from the sandy loam soil were the most resistant to slow wetting and the least resistant to mechanical breakdown, compared to the two other sites. Despite the fairly high uncharred organic carbon content in the sandy loam, the resulting organo-mineral bonds are expected to be weak on coarse-textured soils. This is supported by the observation that the aggregates were able to withstand the least destructive treatment (slow wetting), but not the more destructive ones (fast wetting and mechanical breakdown; Fig. 3).

Regarding the impact of biochar, Juriga and Simanský (2018) identified four mechanisms by which biochar can affect soil aggregate stability. Biochar can (1) modify exchangeable cation contents and pH (Hardy et al., 2016a, 2016b), affecting the flocculation/dispersion processes, (2) interact with mineral soil, including surface hydrophobic-hydrophilic interactions (Joseph et al., 2010; Herath et al., 2013), (3) affect soil biology (Zhang et al., 2018; Li et al., 2020b; Wang et al., 2023), and (4) act as supplemental binding agents in organo-mineral associations (Brodowski et al., 2006; Saran et al., 2009; Burgeon et al., 2021). Therefore, biochar application can increase soil aggregate stability in the short-term, as reported for instance in the review of Blanco-Canqui (2017) and the meta-analysis of Islam et al. (2021). The latter study further highlighted that biochar effects on soil aggregation is context-dependent. Indeed, the effects were higher for biochar derived from wood produced at temperature > 650°C, in field experiments > 3 years and in acidic to neutral pH soils.

Because biochar fragmentation and aging increase its CEC and may therefore enhance its ability to act as a binding agent in soil, we hypothesized that charcoal-C content in kiln sites could improve aggregate

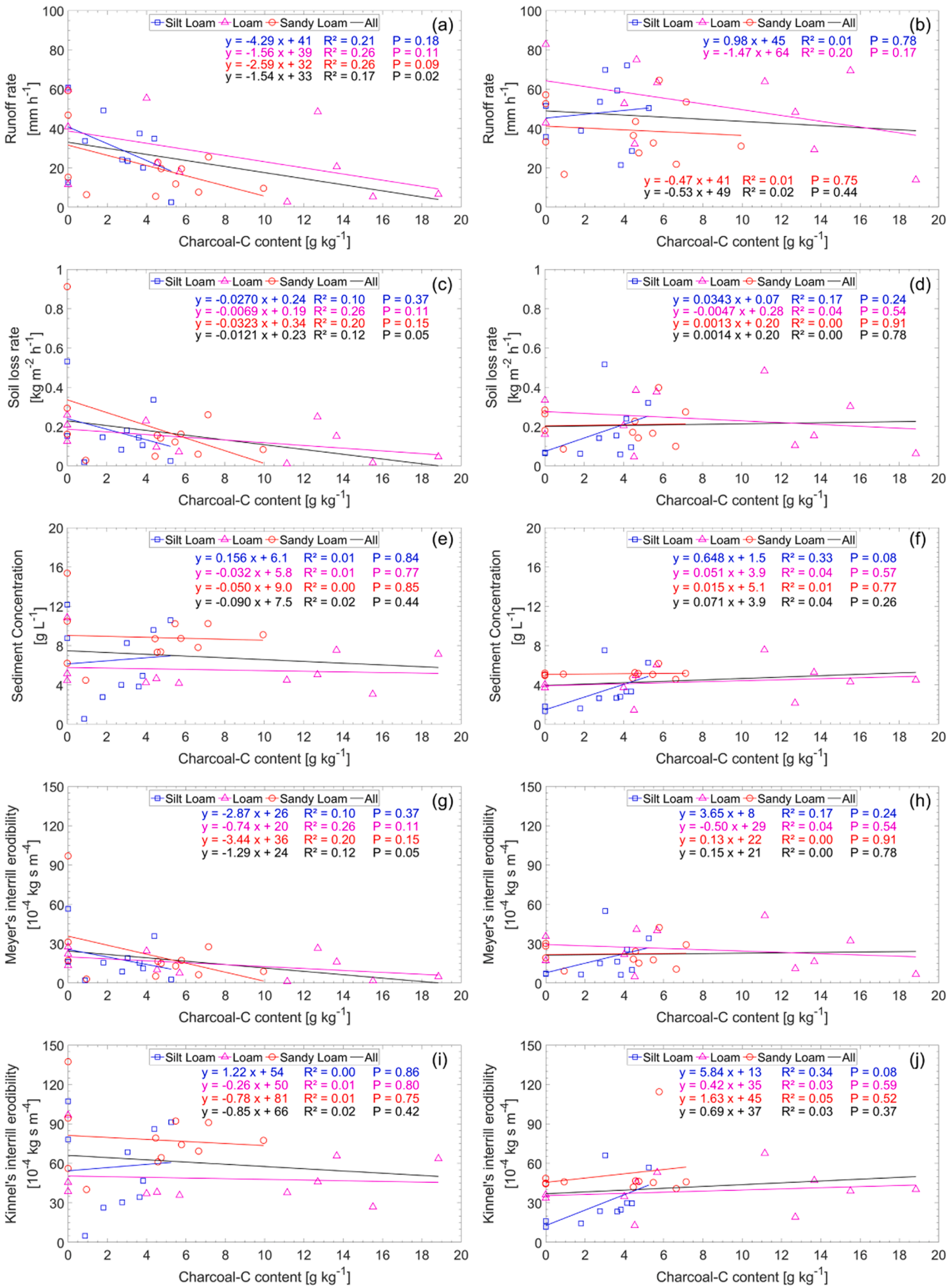

Fig. 6. Relationship between final runoff rate (a, b), final soil loss rate (c, d), sediment concentration (e, f), Meyer's interrill erodibility (g, h) and Kinnel's interrill erodibility (i, j) and the charcoal-C content for the silt loam (Gembloux), loam (Yvoir) and sandy loam (Attert) soils during the first rainfall simulation (a, c, e, g, i) and the second rainfall simulation 24 h later (b, d, f, h, j). "All" corresponds to the linear regression fitted on the data from the three sites combined, and P to the p-value on the slope coefficient of the linear regressions (n=12 per study site).

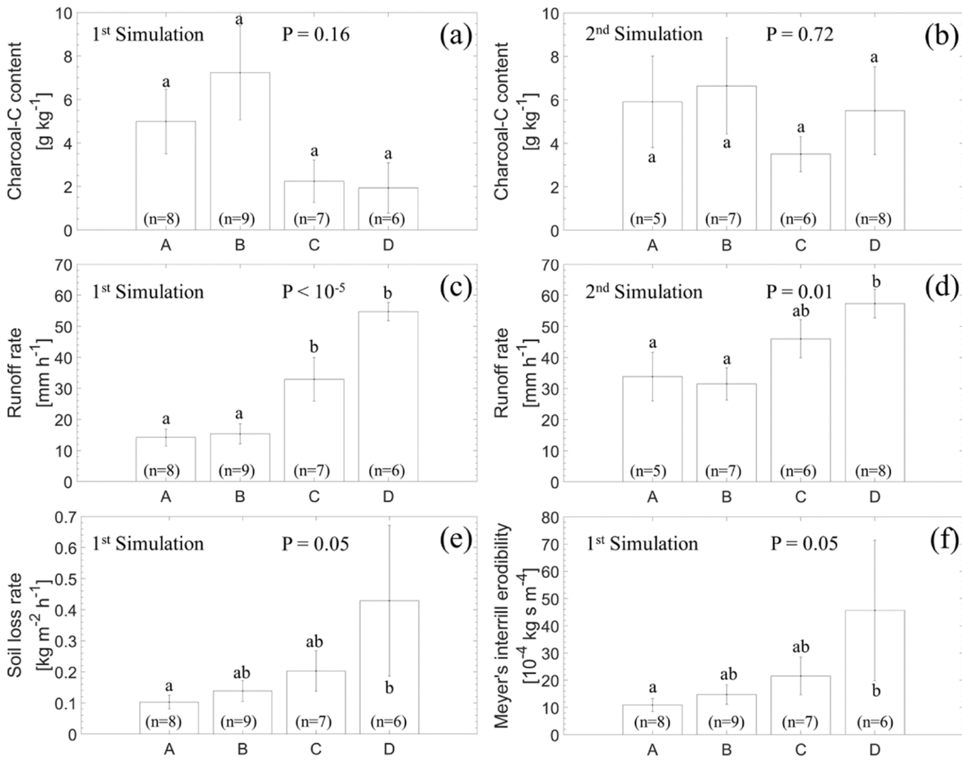

Fig. 7. (a, b) Charcoal-C content, (c, d) final runoff rate, (e) final soil loss rate and (f) Meyer's interrill erodibility for the 4 different groups (A to D) of soil surface conditions at the end of the first (0 h) and second (24 h later) rainfall simulation, all study sites combined. Data are means ± standard errors of the means. P corresponds to the p-value of the ANOVA test. For a given variable, bars marked with different letters are significantly different ($P < 0.05$).

stability mostly through mechanisms (1) and (4). Indeed, charcoal particles were hydrophilic as a result of the aging process (Knicker, 2011; Criscuoli et al., 2014), which excludes mechanism (2), and Hardy et al. (2019) reported a lack of impact of centennial charcoal on soil biological activity in kiln sites, hence mechanisms 3 is not expected to contribute significantly.

Contrary to the initial hypothesis and the literature, we observed a lack of effect of charcoal-C content on soil aggregate stability, irrespective of the study site and aggregate stability test, in spite of the positive effect of charcoal-C on soil chemical properties. Using the same methodology as in the present study, Zanutel and Bielders (2023) also observed a lack of effect of century-old charcoal on aggregate stability in kiln sites on a silt loam soil (a plot different from the present study). However, they reported a positive impact for a sandy loam soil. The latter corresponded to the same field as in the present study, but sampling occurred in early winter 2021 as opposed to early winter 2019 for the present study. Given that the charcoal was present for more than 150 years in the soil, it seems highly unlikely that the difference in outcome between the present study and the study of Zanutel and Bielders (2023) would relate to additional aging (2 years). However, although sampling occurred at approximately the same time of year (early winter) and for similar land use (winter cover crop, preceded by a spring crop), other conditions may have differed that affect aggregate stability. Algayer et al. (2014) for instance demonstrated that moisture content at sampling, antecedent moisture conditions and rain intensity could significantly affect the outcome of the aggregate stability tests. This highlights the need to further investigate the effect of century-old biochar on aggregate stability to arrive at more robust conclusions regarding the conditions (e.g., soil type, moisture content at sampling) under which one may or may not expect a positive effect of century-old biochar on aggregate stability.

Similarly to the present study, several previous studies also did not observe an effect of biochar on aggregate stability (Peng et al., 2011; Borchard et al., 2014; Jeffery et al., 2015; Zhang et al., 2015; Zhou et al., 2019), although all these studies dealt with recent biochar applications. Zhang et al. (2015) attributed the lack of effect of biochar to low application rates (4.5 and 9 t ha^{-1}) and the recent addition (1 year) of biochar to the studied soil. Though consistent with the values reported previously by Hardy et al. (2016b), charcoal-C contents in kiln sites are not very high (1.2–2% at most, depending on the study site), which may limit the ability of charcoal to contribute to aggregate stabilization. Furthermore, Zhou et al. (2019) suggested that biochar carbon is less 'biologically active' than uncharred organic matter and therefore less efficient at binding soil particles or promoting biological activity. The discrepancy between our study and the study of Burgeon et al. (2021) - who observed that century-old charcoal in kiln sites contributes to organo-mineral associations and plays an active role in aggregation patterns - points for the need for further studies. The methodologies used in the study of Burgeon et al. (2021); wet sieving, density fractionation, sonication) and in the present study (slow wetting, fast wetting, mechanical breakdown; Le Bissonnais, 1996) are, however, very different and do not allow for a straightforward comparison.

4.3. Effect of charcoal-C on runoff and interrill soil loss

In this study, we showed that the final runoff and soil loss rates decreased with increasing charcoal-C content during the first rainfall simulation. The reduction of final runoff and soil loss rates as a function of charcoal-C content must, however, be interpreted with some caution, since observations at high charcoal-C contents (> 10 g kg^{-1}) are dominated by a single soil type, i.e., the loamy soil (Fig. 6). Nevertheless, the general trend was also visible for the loamy soil considered alone, which seems to comfort the fact that charcoal-C content may indeed help mitigate runoff and sediment production.

Even though negative or negligible effects of biochar on soil erosion have also been reported previously for short-term studies (e.g., Peng et al., 2016; Li et al., 2017; Lee et al., 2018; Zhang et al., 2019) and in the long-term study of Zanutel and Bielders (2023) on a silt loam soil, a decrease of the final runoff and soil loss rates with increasing charcoal-C content is consistent with some published studies investigating the short-term impact (Khademalrasoul et al., 2019; Li et al., 2019, 2020a; Ahmadi et al., 2020) as well as the long-term impact (for a sandy loam soil; Zanutel and Bielders, 2023) of biochar on soil erosion. More specifically, the review of Blanco-Canqui (2019) revealed a runoff reduction ranging from 5% to 50% on the basis of six studies and a soil loss reduction by 11–78% on the basis of eight studies during rainfall events, whereas the meta-analysis of Gholamahmadi et al. (2023) reported that the application of biochar reduces runoff by 25% and soil loss by 16% on average. These reductions have been attributed to higher aggregate stability and higher permeability following the application of biochar (Li et al., 2019).

In this study, interrill erosion parameters were mostly not significantly related to aggregate stability tests, but to soil surface conditions. However, Fig. 7 shows that soil surface conditions at the end of the rainfall simulations significantly affected both final runoff (1st and 2nd rainfall simulations) and soil loss rates (1st rainfall simulation only). More weakly crusted surfaces with larger numbers of protruding aggregates produced less runoff and sediment than smoother, more severely crusted surfaces. Visual inspection did not reveal an obvious dominance of a certain soil type in a given surface condition class that may have biased the results (i.e., class D was not dominated by samples from the silt loam soil; Figure S1), although a formal verification of independence between soil type and surface conditions by means of a Chi^2 test is not feasible because of too few observations in some combinations (there are too many soil type x surface condition combinations with fewer than 5 observations). The presence of clods in the crust may have increased locally the infiltration (Freebairn et al., 1991) and roughness (Carmi and Berliner, 2008), therefore decreasing the final runoff rate. Since the final soil loss rate is directly related to the final runoff rate (Fig. 5), the reduction of the final soil loss rate during the first rainfall simulation can to a large extent be explained by the reduction of the final runoff rate.

Overall, it thus appears that differences in surface conditions at the end of the rainfall simulations significantly affected final runoff and soil loss rates. Furthermore, charcoal-C contents greater than approx. 5 g kg^{-1} were preferentially associated with surface conditions A and B and with low runoff (and sediment loss rates), at least for the loamy and sandy loam soils (Figure S2). The observed differences in surface conditions at the end of the rainfall simulations could result (1) from differences in soil surface conditions right from the start of the experiment (differences in mean aggregate size at the start of the experiment even though all samples were sieved at < 2 cm; Freebairn et al., 1991; Khademalrasoul, 2019), or (2) from differences in aggregate resistance during rainfall (Le Bissonnais, 1996). Given that aggregate stability was not affected by charcoal-C content and that interrill erosion parameters of the rainfall-runoff experiments were poorly correlated with soil chemical properties, it thus seems that samples rich in charcoal-C may indeed have had a larger mean aggregate size at the start of the experiments. Future studies may seek to confirm this.

The reduction of final runoff and soil loss rates as a function of charcoal-C content observed for the first rainfall experiment was no longer visible for the second rainfall simulation 24 hours later. This lack of effect of charcoal-C for this second rainfall simulation may be explained by considering the kinetics of crust evolution. Freebairn et al. (1991) observed that the clods present in the crust brake down overtime into smaller aggregates, which bridged and blocked voids, thereby further enhancing the crust. Khademalrasoul et al. (2019) similarly observed the presence of clods in biochar-enriched soil, which disintegrated less readily than on the control soil, slowing down the crust formation on the soil with biochar. During the first simulation, the crust may therefore have developed less quickly on charcoal-enriched soils as a result of the presence of more clods, but by the end of the second rainfall simulation, the crust was possibly more equally developed across all samples, irrespective of charcoal-C content. Fig. 8 illustrates clod degradation after the first and second rainfall simulation in a sample from a charcoal kiln site.

4.4. Effect of charcoal-C on interrill erodibility

No standard experimental procedures or set of conditions exist to determine interrill erodibility (Truman and Bradford, 1995). Therefore, interrill erodibility is influenced by the methodology and soil type but also by the type of equation used (Truman and Bradford, 1995). Under transport-limited conditions (Kinnel's equation), the amount of soil loss depends on the ability of the runoff to transport the detached soil particles. Under detachment-limited conditions (Meyer's equation), soil loss rate depends especially on the ability of the rain to detach soil particles. Accordingly, transport-limited conditions dominate at low slope and runoff rates, whereas detachment-limited conditions dominate at high slope and runoff rates.

In this study, the final soil loss rate was linearly related to the final runoff rate (Fig. 5), indicating a prevalence of the transport-limiting conditions. Hence, Kinnel's equation seems better adapted to the conditions of this study. Since the final runoff and soil loss rates decrease to a similar extent with the charcoal-C content, Kinnel's interrill erodibility remains unaffected by the presence of centennial charcoal in kiln sites. The lack of effect of charcoal-C content on Kinnel's interrill erodibility is furthermore consistent with the lack of effect of charcoal-C on aggregate stability in this study.

5. Conclusions

Interrill erosion was studied in centennial charcoal kiln sites on three different soils (silt loam, loam and sandy loam) in Wallonia (Belgium). The presence of century-old charcoal resulted in a significant increase of the cation exchange capacity and the divalent exchangeable cation contents, but ultimately did not affect the aggregate stability, irrespective of the study sites. However, despite the lack of effect on

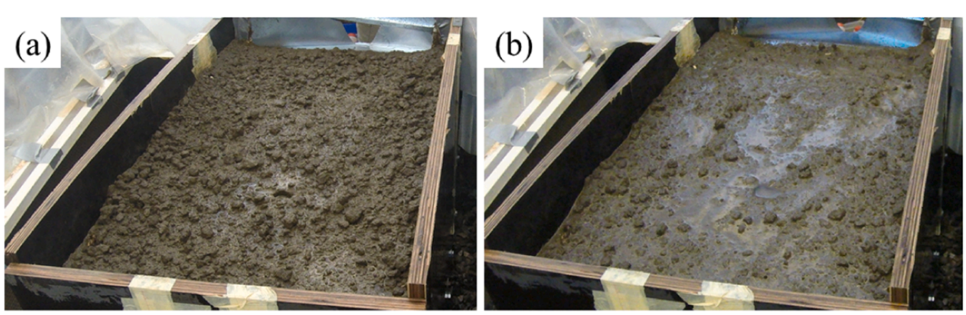

Fig. 8. Illustration of clod degradation during the rainfall simulations for a soil sample from a charcoal kiln site. Photograph of the soil surface condition of the same soil sample after the first (a) and second (b) rainfall simulations. The soil surface after the first rainfall simulation is characterized by the presence of numerous clods which are no longer visible after the second rainfall simulation.

aggregate stability, final runoff and soil loss rates decreased with increasing charcoal-C content. This was attributed to increasing proportions of clods in the soil samples with increasing charcoal-C content, which delayed crust development and maintained a locally higher infiltration rate and roughness in comparison to reference soil samples. The latter was supported by images taken at the end of the rainfall simulations. However, after a second rainfall simulation, these differences were no longer observed, probably because the crust had reached a similar development stage in all treatments.

From a practical point of view, these results seem to indicate that the benefits of century-old biochar for soil erosion control may be limited to the first weeks or months after tillage, with a threshold cumulative rainfall value after which no further benefits are to be expected (until the next tillage operation). This assumes that clod-size distribution in the seedbed after tillage depends on charcoal-C content. The resulting cumulative rainfall threshold value is then also expected to be dependent on charcoal-C content. Despite its temporary nature, this beneficial effect may be beneficial since it acts at a time when vegetation cover is at its lowest (i.e., immediately after tillage and seedbed preparation). Further research on a wider variety of soils would nevertheless be warranted to confirm the observed trends and to further test the hypothesis of clod stabilization by the presence of century-old charcoal.

Data Availability

Data will be made available on request.

Acknowledgements

This work is part of a Ph.D. supported by a FRIA grant from the Belgian Fund for Scientific Research (FSR-FNRS; grant number: FC036167).

Appendix A. Supporting information

Supplementary data associated with this article can be found in the online version at doi:10.1016/j.still.2024.106091.

References

Ahmadi, S.H., Ghasemi, H., Sepaskhah, A.R., 2020. Rice husk biochar influences runoff features, soil loss, and hydrological behavior of a loamy soil in a series of successive simulated rainfall events. Catena 192, 104587. https://doi.org/10.1016/j.catena.2020.104587.

Algayer, B., Le Bissonnais, Y., Darboux, F., 2014. Short-term dynamics of soil aggregate stability in the field. Soil Sci. Soc. Am. J. 78, 1168–1176. https://doi.org/10.2136/sssaj2014.01.0009.

Assouline, S., Ben-Hur, M., 2006. Effects of rainfall intensity and slope gradient on the dynamic of interrill erosion during soil surface sealing. Catena 66, 211–220. https://doi.org/10.1016/j.catena.2006.02.005.

Auzet, A.V., Boiffin, J., Ludwig, B., 1995. Concentrated flow erosion in cultivated catchments: Influence of soil surface state. Earth Surf. Proccess. Landf. 20, 759–767. https://doi.org/10.1002/esp.3290200807.

Auzet, A.V., van Dijk, P., Kirkby, M.J., 2005. Surface characterization for soil erosion forecasting. Catena 62, 77–78. https://doi.org/10.1016/j.catena.2005.05.009.

Biederman, L.A., Harpole, W.S., 2013. Biochar and its effects on plant productivity and nutrient cycling: a meta-analysis. Glob. Change Biol. Bioenergy 5, 202–214. https://doi.org/10.1111/gcbb.12037.

Bielders, C.L., Ramelot, C., Persoons, E., 2003. Farmer perception of runoff and erosion and extent of flooding in the silt-loam belt of the Belgian Walloon Region. Environ. Sci. Policy 6, 85–93 https://doi.org/10.1016/S1462-9011(02)00117-X.

Blanco-Canqui, H., 2017. Biochar and Soil Physical Properties. Soil Sci. Soc. Am. J. 81, 687–711. https://doi.org/10.2136/sssaj2017.01.0017.

Blanco-Canqui, H., 2019. Biochar and water quality. J. Environ. Qual. 48, 2–15. https://doi.org/10.2134/jeq2018.06.0248.

Boardman, J., Poesen, J., 2006. Soil Erosion in Europe: Major Processes, Causes and Consequences. In: Soil erosion in Europe (Eds. J. Boardman and J. Poesen). Wiley, Chichester, 477-487. https://doi.org/10.1002/0470859202.ch36.

Boardman, J., Verstraeten, G., Bielders, C., 2006. Muddy floods. In: Soil erosion in Europe (Eds. J. Boardman and J. Poesen). Wiley, Chichester, 743-755. https://doi.org/10.1002/0470859202.ch53.

Borchard, N., Siemens, J., Ladd, J.B., Möller, A., Amelung, W., 2014. Application of biochars to sandy and silty soil failed to increase maize yield under common agricultural practice. Soil Tillage Res 144, 184–194. https://doi.org/10.1016/j.still.2014.07.016.

Brodowski, S., John, B., Flessa, H., Amelung, W., 2006. Aggregate-occluded black carbon in soil. Eur. J. Soil Sci. 57, 539–546. https://doi.org/10.1111/j.1365-2389.2006.00807.x.

Bronick, C.J., Lal, R., 2005. Soil structure and management: A review. Geoderma 124, 3–22. https://doi.org/10.1016/j. geoderma.2004.03.005.

Burgeon, V., Fouché, J., Leifeld, J., Chenu, C., Cornelis, J.-T., 2021. Organo-mineral associations largely contribute to the stabilization of century-old pyrogenic organic matter in cropland soils. Geoderma, 114841. https://doi.org/10.1016/j.geoderma.2020.114841.

Carmi, G., Berliner, P., 2008. The effect of soil crust on the generation of runoff on small plots in an arid environment. Catena 74, 37–42. https://doi.org/10.1016/j.catena.2008.02.002.

Cerdan, O., Souchère, V., Lecomte, V., Couturier, A., Le Bissonnais, Y., 2002. Incorporating soil surface crusting processes in an expert-based runoff model: Sealing and Transfer by Runoff and Erosion related to Agricultural Management. Catena 46, 189–205. https://doi.org/10.1016/S0341-8162(01)00166-7.

Cheng, C.-H., Lehmann, J., Thies, J.E., Burton, S.D., Engelhard, M.H., 2006. Oxidation of black carbon by biotic and abiotic processes. Org. Geochem. 37, 1477–1488. https://doi.org/10.1016/j.orggeochem.2006.06.022.

Cheng, C.-H., Lehmann, J., Engelhard, M.H., 2008. Natural oxidation of black carbon in soils: Changes in molecular form and surface charge along a climosequence. Geochim. Cosmochim. Acta 72, 1598–1610. https://doi.org/10.1016/j.gca.2008.01.010.

Chenu, C., Le Bissonnais, Y., Arrouays, D., 2000. Organic matter influence on clay wettability and soil aggregate stability. J. Soil Water Conserv. 64, 1479–1486. https://doi.org/10.2136/sssaj2000.6441479x.

Criscuoli, I., Alberti, G., Baronti, S., Favilli, F., Martinez, C., Calzolari, C., Pusceddu, E., Rumpel, C., Viola, R., Miglietta, F., 2014. Carbon sequestration and fertility after centennial time scale incorporation of charcoal into soil. PloS One 9, 1–11. https://doi.org/10.1371/journal.pone.0091114.

Ding, Y., Liu, Y., Liu, S., Li, Z., Tan, X., Huang, X., Zeng, G., Zhou, L., Zheng, B., 2016. Biochar to improve soil fertility. A review. Agron. Sustain. Dev. 36, 1–18. https://doi.org/10.1007/s13593-016-0372-z.

Evrard, O., Bielders, C.L., Vandaele, K., Van Wesemael, B., 2007. Spatial and temporal variation of muddy floods in central Belgium, offsite impacts and potential control measures. Catena 70, 443–454. https://doi.org/10.1016/j.catena.2006.11.011.

Evrard, O., Heitz, C., Liégeois, M., Boardman, J., Vandaele, K., Auzet, A.-B., Van Wesemael, B., 2010. A comparison of management approaches to control muddy floods in central Belgium, northern France and southern England. Land. Degrad. Dev. 21, 322–335. https://doi.org/10.1002/ldr.1006.

Freebairn, D.M., Gupta, S.C., Rawls, W.J., 1991. Influence of Aggregate Size and Microrelief on Development of Surface Soil Crusts. Soil Sci. Soc. Am. J. 55, 188–195. https://doi.org/10.2136/sssaj1991.03615995005500010033x.

Gholamahmadi, B., Jeffery, S., Gonzalez-Pelayo, O., Prats, S.A., Bastos, A.C., Keizer, J.J., Verheijen, F.G.A., 2023. Biochar impacts on runoff and soil erosion by water: A systematic global scale meta-analysis. Sci. Total Environ. 871, 161860 https://doi.org/10.1016/j.scitotenv.2023.161860.

Guo, T., Wang, Q., Li, D., Wu, L., 2010. Sediment and solute transport on soil slope under simultaneous influence of rainfall impact and scouring flow. Hydrol. Process. 24, 1146–1454. https://doi.org/10.1002/hyp.7605.

Gupta, D.K., Gupta, C.K., Dubey, R., Fagodiya, R.K., Sharma, G., Keerthika, A., Mohamed, M.B.N., Dev, R., Shukla, A.K., 2020. Role of Biochar in Carbon Sequestration and Greenhouse Gas Mitigation. In: Singh, J., Singh, C. (Eds.), In: Biochar Applications in Agriculture an Environment Management. Springer, Cham.

Hardy, B., Dufey, J., 2012. Estimation des besoins en charbon de bois et en superficie forestierepour la siderurgie wallonne preindustrielle (1750–1830) deuxième partie: les besoins en superficie forestiere. Rev. . Française 6, 799–806.

Hardy, B., Dufey, J., 2015. Les aires de faulde en forêt wallonne: repérage, morphologie et distribution spatiale. êt Nat. 135, 20–30.

Hardy, B., Cornelis, J.-T., Houben, D., Leifeld, J., Lambert, R., Dufey, J.E., 2016b. Evaluation of the long-term effect of biochar on properties of temperate agricultural soil at pre-industrial charcoal kiln sites in Wallonia, Belgium. Eur. J. Soil Sci. 68, 80–89. https://doi.org/10.1111/ejss.12395.

Hardy, B., Cornelis, J.-T., Houben, D., Lambert, R., Dufey, J.E., 2016a. The effect of pre-industrial charcoal kilns on chemical properties of forest soil of Wallonia, Belgium. Eur. J. Soil Sci. 67, 206–216. https://doi.org/10.1111/ejss.12324.

Hardy, B., Leifeld, J., Knicker, H., Dufey, J.E., Deforce, K., Cornelis, J.-T., 2017. Long term change in chemical properties of preindustrial charcoal particles aged in forest and agricultural temperate soil. Org. Geochem. 107, 33–45. https://doi.org/10.1016/j.orggeochem.2017.02.008.

Hardy, B., Sleutel, S., Dufey, J.E., Cornelis, J.-T., 2019. The Long-Term effect of Biochar on Soil Microbial Abundance, Activity and Community Structure Is Overwritten by Land Management. Front. Environ. Sci. 7, 110. https://doi.org/10.3389/fenvs.2019.00110.

Herath, H.M.S.K., Camps-Arbestain, M., Hedley, M., 2013. Effect of biochar on soil physical properties in two contrasting soils: an Alfisol and an Andisol. Geoderma 209–210 188–197. https://doi.org/10.1016/j.geoderma.2013.06.016.

Hernandez-Soriano, M.C., Kerré, B., Goos, P., Hardy, B., Duféy, J., Smolders, E., 2016. Long-term effect of biochar on the stabilization of recent carbon: soils with historical inputs of charcoal. Glob. Change Biol. Bioenergy 8, 371–381. https://doi.org/10.1111/gcbb.12250.

Islam, M.U., Jiang, F., Guo, Z., Peng, X., 2021. Does biochar application improve soil aggregation? A meta-analysis. Soil Tillage Res 209, 104926. https://doi.org/10.1016/j.still.2020.104926.

Jeffery, S., Verheijen, F.G.A., van der Velde, M., Bastos, A.C., 2011. A quantitative review of the effects of biochar application to soils on crop productivity using meta-analysis. Agric. Ecosyst. Environ. 144, 175–187. https://doi.org/10.1016/j.agee.2011.08.015.
Jeffery, S., Meinders, M.B.J., Stoof, C.R., Bezemer, T.M., van de Voorde, T.F.J., Mommer, L., van Groenigen, J.W., 2015. Biochar application does not improve the soil hydrological function of a sandy soil, 251-252 Geoderma 47–54. https://doi.org/10.1016/j. geoderma.2015.03.022.
Joseph, S.D., Camps-Arbestain, M., Lin, Y., Munroe, P., Chia, C.H., Hook, J., van Zwieten, L., Kimber, S., Cowie, A., Singh, B.P., Lehmann, J., Foidl, N., Smernik, R.J., Amonette, J.E., 2010. An investigation into the reactions of biochar in soil. Soil Res 48, 501–515. https://doi.org/10.1071/SR10009.
Juriga, M., Simanský, V., 2018. Effect of biochar on soil structure – review. Acta Fytotech. Zootech. 21, 11–19. https://doi.org/10.15414/afz.2018.21.01.11-19.
Khademalrasoul, A., Kuhn, N.J., Elsgaard, L., Hu, Y., Iversen, B.V., Heckrath, G., 2019. Short-term effects of biochar application on soil loss during a rainfall-runoff simulation. Soil Sci. 184, 17–24. https://doi.org/10.1097/SS.0000000000000247.
Kinnel, P.I.A., 1993. Interrill erodibilities based on the rainfall intensity-flow discharge erosivity factor. Aus. J. Soil Res 31, 319–332. https://doi.org/10.1071/sr9930319.
Knicker, H., 2011. Pyrogenic organic matter in soil: Its origin and occurrence, its chemistry and survival in soil environments. Quat. Int. 243, 251–263. https://doi.org/10.1016/j.quaint.2011.02.037.
Lakanen, E., Erviö, R., 1971. A comparison of eight extractants for the determination of plant available micronutrients in soils. Acta Agral. Fenn. 123, 223–232.
Laloy, E., Bielders, C., 2010. Effect of Intercropping Period Management on Runoff and Erosion in a Maize Cropping System. J. Environ. Qual. 39, 1001–1008. https://doi.org/10.2134/jeq2009.0239.
Le Bissonnais, Y., 1996. Aggregate stability and assessment of soil crustability and erodibility: I. theory and methodology. Eur. J. Soil Sci. 47, 425–437. https://doi.org/10.1111/ejss.4_12311.
Lee, C.-H., Wang, C.-C., Lin, H.-H., Lee, S.S., Tsang, D., Jien, S.-H., Ok, Y.S., 2018. In-situ biochar application conserves nutrients while simultaneously mitigating runoff and erosion of an Fe-oxide-enriched tropical soil, 619-620 Sci. Total Environ. 665–671. https://doi.org/10.1016/j.scitotenv.2017.11.023.
Lehmann, J., 2007. A handful of carbon. Nature 447, 10–11. https://doi.org/10.1038/447143a.
Lehmann, J., Joseph, S., 2015. Biochar for Environmental Management: An Introduction. In: Lehmann, J., Joseph, S. (Eds.), In: Biochar for Environmental Management. Science and Technology, Londen.
Lehmann, J., Liang, B., Solomon, D., Lerotic, M., Luizão, F., Kinyangi, J., Schäfer, T., Wirick, S., Jacobsen, C., 2005. Near-edge X-ray absorption fine structure (NEXAFS) spectroscopy for mapping nano-scale distribution of organic carbon forms in soil: application to black carbon particles. Glob. Biogeochem. Cycles 19, GB1013. https://doi.org/10.1029/2004GB002435.
Lehmann, J., Gaunt, J., Rondon, M., 2006. Bio-char sequestration in terrestrial ecosystems – a review. Mitig. Adapt. Strateg. Glob. Chang. 11, 395–419. https://doi.org/10.1007/s11027-005-9006-5.
Li, X., Wang, T., Chang, S.X., Jiang, X., Song, Y., 2020b. Biochar increases soil microbial biomass but has variable effects on microbial diversity: a meta-analysis. Sci. Total Environ. 749, 141593 https://doi.org/10.1016/j.scitotenv.2020.141593.
Li, Y., Zhang, F., Yang, M., Zhang, J., Xie, Y., 2019. Impacts of biochar application rates and particle sizes on runoff and soil loss in small cultivated loess plots under simulated rainfall. Sci. Total. Environ. 649, 1403–1413. https://doi.org/10.1016/j.scitotenv.2018.08.415.
Li, Y., Feng, G., Tewolde, H., Yang, M., Zhang, F., 2020a. Soil, biochar, and nitrogen loss to runoff from loess soil amended with biochar under simulated rainfall. J. Hydrol. 591, 125318 https://doi.org/10.1016/j.jhydrol.2020.125318.
Li, Z.G., Gu, C.M., Zhang, R.H., Ibrahim, M., Zhang, G.S., Wang, L., Zhang, R.Q., Chen, F., Liu, Y., 2017. The benefic effect induced by biochar on soil erosion and nutrient loss of slopping land under natural rainfall conditions in central China. Agric. Water Manag. 185, 145–150. https://doi.org/10.1016/j.agwat.2017.02.018.
Liebenow, A.M., Elliot, W.J., Laflen, J.M., Kohl, K.D., 1990. Interrill erodibility: collection and analysis of data from cropland soils. Trans. ASAE 33, 1882–1888. https://doi.org/10.13031/2013.31553.
Maetens, W., Poesen, J., Vanmaercke, M., 2012. How effective are soil conservation techniques in reducing plot runoff and soil loss in Europe and the Mediterranean? Earth Sci. Rev. 115, 21–36. https://doi.org/10.1016/j.earscirev.2012.08.003.
Malet, J.-P., Auzet, A.-V., Maquaire, O., Ambroise, B., Descroix, L., Esteves, M., Vandervaere, J.-P., Truchet, E., 2003. Soil surface characteristics influence on infiltration in black marls: Application to the Super-Sauze earthflow (southern Alps, France). Earth Surf. Process. Landf. 28, 547–564. https://doi.org/10.1002/esp.457.
Meyer, L.D., 1981. How rain intensity affects interrill erosion. Trans. ASAE 24, 1472–1475. https://doi.org/10.13031/2013.34475.
Palansooriya, K.N., Ok, Y.S., Awad, Y.M., Lee, S.S., Sung, J.-K., Koutsospyros, A., Moon, D.H., 2019. Impacts of biochar application on upland agriculture: A review. J. Environ. Manag. 234, 52–64. https://doi.org/10.1016/j.jenvman.2018.12.085.
Panagos, P., Standardi, G., Borrelli, Lugato, E., Montanarella, L., Bosello, F., 2017. Cost of agricultural productivity loss due to soil erosion in the European Union: From direct cost evaluation approaches to the use of macroeconomic models. Land Degrad. Dev. 29, 471–484. https://doi.org/10.1002/ldr.2879.
Peng, X., Ye, L.L., Wang, C.H., Sun, B., 2011. Temperature- and duration-dependent rice straw-derived biochar: Characteristics and its effects on soil properties of an Ultisol in southern China. Soil Tillage Res 112, 159–166. https://doi.org/10.1016/j.still.2011.01.002.
Peng, X., Zhu, Q.H., Xie, Z.B., Darboux, F., Holden, N.M., 2016. The impact of manure, straw and biochar amendments on aggregation and erosion in a hillslope Ultisol. Catena 138, 30–37. https://doi.org/10.1016/j.catena.2015.11.008.
Rivera, J.I., Bonilla, C.A., 2020. Predicting soil aggregate stability using readily available soil properties and machine learning techniques. Catena 187, 104408. https://doi.org/10.1016/j.catena.2019.104408.
Saran, S., Elisa, L.C., Evelyn, K., Roland, B., 2009. Biochar, climate change and soil: A review to guide future research. In: E. Krull (ed.), Csiro Land and Water Science Report 05/09, 23.
Singh, H., Northup, B.K., Rice, C.W., Prasad, P.V., 2022. Biochar applications influence soil physical and chemical properties, microbial diversity, and crop productivity: a meta-analysis. Biochar 4, 8 https://doi.org/10.1007/s42773-022-00138-1.
Singh, N., Abiven, S., Torn, M.S., Schmidt, M.W.I., 2012. Fire-derived organic carbon in soil turns over on a centennial scale. Biogeosciences 9, 2847–2857. https://doi.org/10.5194/bg-9-2847-2012.
Solomon, D., Lehmann, J., Thies, J., Schäfer, T., Liang, B., Kinyangi, J., Neves, E., Petersen, J., Luizão, F., Skjemstad, J., 2007. Molecular signature and sources of biochemical recalcitrance of organic C in Amazonian Dark Earths. Geochim. Et. Cosmochim. Acta 71, 2285–2298. https://doi.org/10.1016/j.gca.2007.02.014.
Truman, C.C., Bradford, J.M., 1995. Laboratory Determination of Interrill Soil Erodibility. Soil Sci. Soc. Am. J. 59, 519–526. https://doi.org/10.2136/sssaj1995.03615995005900020035x.
Trupiano, D., Cocozza, C., Baronti, S., Amendola, C., Vaccari, F.P., Lustrato, G., Di Lonardo, S., Fantasma, F., Tognetti, R., Scippa, G.S., 2017. The effects of biochar and its combination with compost on lettuce (Lactuca sativa L.) growth, soil properties, and soil microbial activity and abundance. Int. J. Agron. 2017, 1–12. https://doi.org/10.1155/2017/3158207.
Verstraeten, G., Poesen, J., 1999. The nature of small-scale flooding, muddy floods and retention pond sedimentation in central Belgium. Geomorphology 29, 275–292. https://doi.org/10.1016/S0169-555X(99)00020-3.
Verstraeten, G., Poesen, J., Govers, G., Gillijns, K., Bielders, C., Goossens, D., Ruysschaert, G., Van Den Eeckhaut, M., Vanwalleghem, T., 2006. Soil erosion in Belgium. In: J. Boardman and J. Poesen (eds). Soil erosion in Europe. Wiley, Chichester, pp. 385-411.
Wang, M., Yu, X., Weng, X., Zeng, X., Li, M., Sui, W., 2023. Meta-Analysis of the Effects of Biochar Application on the Diversity of Soil Bacteria and Fungi. Microorganisms 11, 641. https://doi.org/10.3390/microorganisms11030641.
Woolf, D., Amonette, J.E., Street-Perrott, F.A., Lehmann, J., Joseph, S., 2010. Sustainable biochar to mitigate global climate change. Nat. Commun. 1, 56. https://doi.org/10.1038/ncomms1053.
Zanutel, M., Bielders, C., 2023. Contrasted effects of biochar application on interrill erosion depending on age, application rate and soil type. Geoderma Reg. 34 e00706.
Zanutel, M., Garré, S., Bielders, C., 2021. Long-term effect of biochar on physical properties of agricultural soils with different textures at pre-industrial charcoal kiln sites in Wallonia (Belgium). Eur. J. Soil Sci. 73, 1–17. https://doi.org/10.1111/ejss.13157.
Zhang, F., Huang, C., Yang, M.-Y., Zhang, J., Shi, W., 2019. Rainfall simulation experiments indicate that biochar addition enhances erosion of loess-derived soils. Land Degrad. Dev. 30, 1–15. https://doi.org/10.1002/ldr.3399.
Zhang, L., Jing, Y., Xiang, Y., Zhang, R., Lu, H., 2018. Responses of soil microbial community structure changes and activities to biochar addition: a meta-analysis. Sci. Total Environ. 643, 926–935. https://doi.org/10.1016/j.scitotenv.2018.06.231.
Zhang, Q., Du, Z.L., Lou, Y., He, X., 2015. A one-year short-term biochar application improved carbon accumulation in large macroaggregate fractions. Catena 127, 26–31. https://doi.org/10.1016/j.catena.2014.12.009.
Zhang, X.C., Zheng, F.L., Chen, J., Garbrecht, J.D., 2020. Characterizing detachment and transport of interrill soil erosion. Geoderma 376, 114549. https://doi.org/10.1016/j.geoderma.2020.114549.
Zhao, Q., Li, D., Zhuo, M., Guo, T., Liao, Y., Xie, Z., 2015. Effects of rainfall intensity and slope gradient on erosion characteristics of the red soil slope. Stoch. Environ. Res. Risk Assess. 29, 609–621. https://doi.org/10.1007/s00477-014-0896-1.
Zhou, H., Fang, H., Zhang, Q., Wang, Q., Chen, C., Mooney, S.J., Peng, X., Du, Z., 2019. Biochar enhances soil hydraulic function but not soil aggregation in a sandy loam. Eur. J. Soil Sci. 70, 291–300. https://doi.org/10.1111/ejss.12732.
Zuazo, V.H.D., Pleguezuelo, C.R.R., 2008. Soil-Erosion and runoff prevention by plant covers: a review. Agron. Sustain. Dev. 28, 65–86. https://doi.org/10.1051/agro:2007062.